Feature-Based 3D Reconstruction Model for Close-Range Objects and Its Application to Human Finger

Feng Liu[1(✉)], Linlin Shen[1], and David Zhang[2]

[1] School of Computer Science & Software Engineering, Computer Vision Institute, Shenzhen University, Shenzhen, China
feng.liu@szu.edu.cn

[2] Department of Computing, The Hong Kong Polytechnic University, Hung Hom, Kowloon, Hong Kong, China

Abstract. This paper addresses the problem of feature-based 3D reconstruction model for close-range objects. Since it is almost impossible to find pixel-to-pixel correspondences from 2D images by algorithms when the object is imaged on a close range, the selection of feature correspondences, as well as the number and distribution of them, play important roles in the reconstruction accuracy. Then, features on representative objects are analyzed and discussed. The impact of the number and distribution of feature correspondences is analyzed by reconstructing an object with standard cylinder shape by following the reconstruction model introduced in the paper. After that, three criteria are set to guide the selection of feature correspondences for more accurate 3D reconstruction. These criteria are finally applied to the human finger since it is a typical close-range object and different number and distribution of feature correspondences can be established automatically from its 2D fingerprints. The effectiveness of the setting criteria is demonstrated by comparing the accuracy of reconstructed finger shape based on different fingerprint feature correspondences with the corresponding 3D point cloud data obtained by structured light illumination (SLI) technique which is taken as a ground truth in the paper.

1 Introduction

The 3D geometric shape and appearance of objects offer attributes that are invariant to the changes introduced by the imaging process. These attributes can facilitate recognition and assist in various applications, including graphical animation, medical applications, and so forth. Thus, how to obtain the 3D geometric models of real objects has attracted more and more attentions from researchers and companies [1-18]. In computer vision and computer graphics, the process of capturing the shape and appearance of real objects refers to 3D reconstruction. Currently, the existing 3D reconstruction techniques are divided into two categories: active and passive modeling. Active modeling creates the 3D point cloud data of geometric surface by interfering with the reconstructed objects, either mechanically or radiometrically [1-6], while the passive modeling uses only the information contained in the images of the scene to generate the 3D information, namely image-based reconstruction [7-17]. Each of these

H. Zha et al. (Eds.): CCCV 2015, Part II, CCIS 547, pp. 379–393, 2015.
DOI: 10.1007/978-3-662-48570-5_37

two kinds of modeling has its own advantages and disadvantages. The active modeling reconstructs the 3D model of objects by devices directly with high accuracy but the used devices are costly and cumbersome [18]. The image-based reconstruction generates the 3D model of objects based on their 2D plain images captured by cameras which are challenged to achieve high reconstruction accuracy but the adopted capturing devices (cameras) are usually cheap and light weight [19]. Considering the cost and portability, as well as aiming to make breakthroughs to the reconstruction accuracy, image-based reconstruction is deeply investigated, as summarized in [20, 21].

As summarized in [20], there are mainly five kinds of image-based reconstruction methods: shape from shading [7-9], photometric stereo [14-16], stereopsis [10,11], photogrammetry [22-24], and shape from video [12,13]. The shape-from-shading approaches recover the shape of an object from a gradual variation of shading in the image and only one 2D image is needed for depth calculation. Thus, they are the least on equipment requirements but at the price of accuracy and computational complexity [25]. Photometric stereo methods measure 3D coordinates based on different images of the object's surface taken under multiple non-collinear light sources. This kind of methods is an improved version of the shape from shading ones. Higher reconstruction accuracy is achieved due to the usage of more light sources and images [20]. The stereopsis approaches calculate the 3D depth by binocular disparity and two different images captured at the same time are necessary for 3D depth computation. This kind of methods provides better accuracy with less mathematical complexity but difficulty lies in establishing of feature correspondences in two different images automatically and making essential equipment calibrations [26]. Photogrammetry approaches use the same methods to compute the 3D coordinates as the stereopsis ones. Thus, they have similar merits and drawbacks. But, photogrammetry approaches usually use more than two images and produces good results in some types of applications. Typically, they have been successfully applied for modeling archaeological and architectural objects [20]. The shape-from-video approaches render the assumptions in all previous methods since a series of images can be parted from a video. But the problem still lies in the establishment of correspondences from 2D plain images. This kind of methods is usually used in reconstructing terrain, natural targets and buildings [21]. Among all of those methods, photogrammetry approaches are classical and well established ones. They have been around since nearly the same time as the discovery of photography itself [27]. Whereas, photogrammetrists are usually interested in building detailed and accurate 3D models from images. However, in the field of computer vision, work is being done on automating the reconstruction problem and implementing an intelligent human-like system that is capable of extracting relevant information from image data [28]. Thus, algorithms are usually specifically designed for different applications. Currently, the applications of 3D reconstruction approaches are mainly focus on the modeling of terrain, natural targets, as well as archaeological and architectural objects. The characteristics of those kinds of objects are imaged at a long distance and have contour points, as the examples shown in Fig. 1. The reconstruction of these kinds of objects made researchers ignored two important problems met by the reconstruction of close-range objects: one is that it is hard to find contour points or corner points for correspondences establishment on their 2D plain images of the close-range objects, the influence of the selection of feature correspondences, as well as the number of correspondences is increased for the reconstruction of close-range objects. The other one is minor depth difference corresponds to a significant rise of pixel difference on 2D plain images for the reconstruction of close-range objects. The effect of the distribution of correspondences is enlarged in this situation.

Currently, there are no proven results for close-range objects and irregular surfaces like human biometrics (see Fig. 2). Motivated by designing an effective method to model the shape of close-range objects without contour correspondences, a feature-based 3D reconstruction model is investigated in this paper. This 3D modeling was on the base of traditional binocular stereo vision theory. The methodology of the used reconstruction method is first introduced in this paper. Then, for the first time we analyzed the selection of feature points for correspondence establishment for close-range objects, as well as the impact of the number and distribution of feature correspondences on reconstruction accuracy by reconstructing an object with standard cylinder shape and of radius 10mm. The number and distribution of correspondences from two pictures of the cylinder were labeled and selected manually. After that, three criteria were set to guide the selection of feature correspondences on close-range objects for more accurate 3D reconstruction. These criteria were finally applied to the human finger since it is a typical close-range object and different number and distribution of feature correspondences can be established automatically from its 2D fingerprints. The effectiveness of the setting criteria was demonstrated by comparing the accuracy of reconstructed finger shape based on different fingerprint feature correspondences with the corresponding 3D point cloud data obtained by structured light illumination (SLI) technique which was taken as a ground truth in the paper.

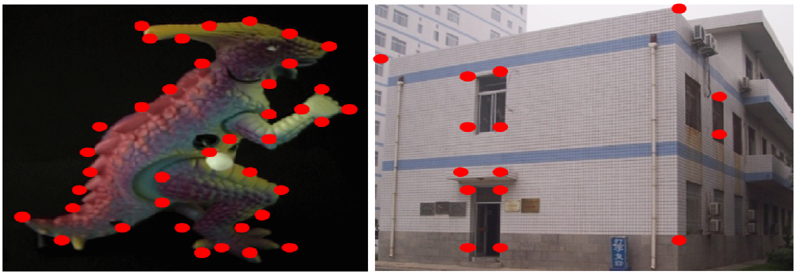

(a) (b)

Fig. 1. Example images of archaeological and architectural objects labeled with contour points, (a) dinosaur, (b) buildings.

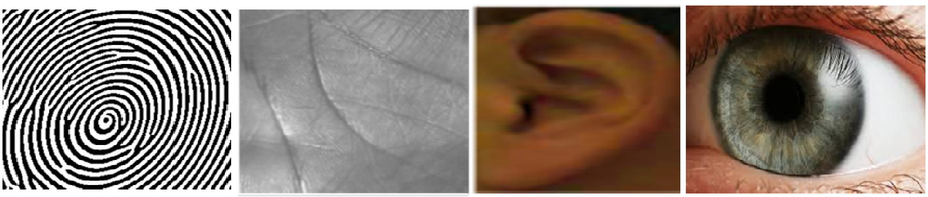

(a) (b) (c) (d)

Fig. 2. Example images of close-range small objects, (a) finger, (b) palm, (c) ear, (d) iris.

2 Feature-Based 3D Reconstruction Model

Based on the theory of binocular stereo vision [29], the 3D information of an object can be obtained from its two different plane pictures captured at one time. As shown in Fig. 3, given two images C_l and C_r simultaneously captured from two viewpoints, the 3D coordinate of V can be calculated if some camera parameters (e.g., focal length of the left camera f_l, focal length of the right camera f_r, principal point of the left camera O_l, principal point of the right camera O_r) and the matched pair $((v_l(x_l, y_l)) \leftrightarrow (v_r(x_r, y_r))$, where $v_*(*)$ represents a 2D point in the given images C_l or C_r ; x_* is the column-axis of the 2D image, and y_* is the row-axis of the 2D image) are provided. Thus, there are mainly three steps to obtain the 3D space coordinate of points from 2D images, namely camera calculation, correspondence establishment, and 3D coordinates calculation.

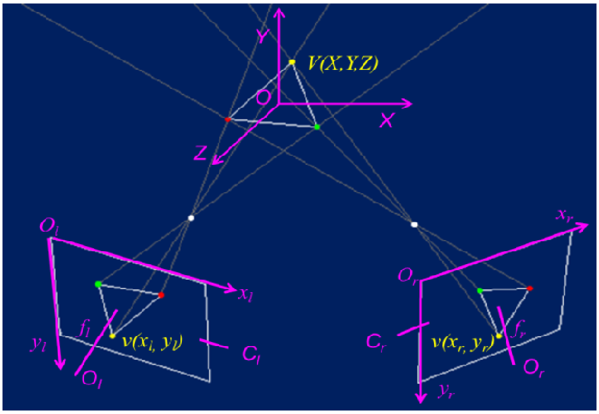

Fig. 3. 3D coordinates calculation on 3D space using binocular stereo vision theory.

Camera calibration refers to the calculation of camera parameters. It is the first step of reconstruction and provides the intrinsic parameters (focal length, principal point, skew, and distortion) of each camera and extrinsic parameters (rotation, translation) between cameras necessary for reconstruction. It usually implements off-line and the commonly used methods and codes are available [30, 31].

Correspondence establishment is of great importance and also a huge challenging problem to 3D modeling. The methods for correspondence establishment are categorized into two classes: feature-based approach and correlation technique [32-34]. Feature-based approach usually produces sparse depth maps by matching feature correspondences while correlation technique yields to dense depth maps by matching all pixels in the entire images. Each has merits and drawbacks. Feature-based approach is suitable when good features can be extracted from 2D images, relatively insensitive to illumination changes and faster than correlation technique. But it usually just provides sparse depth maps. While correlation technique is easier to implement than feature-based method and can provide a dense depth map. It does not work well when viewpoints are very different. Generally, feature-based approach is preferable than correlation technique by taking both accuracy and time complexity into account.

The 3D coordinate of each correspondence can be calculated by using the stereo triangulation method when given camera parameters and matched pairs between images of different views [31].

However, to obtain the 3D surface of an object, it is necessary to produce dense depth maps. They are two ways to realize 3D surface reconstruction by feature-based approach. One is to establish pixel-to-pixel correspondence by estimating the transformation model between 2D images based on feature correspondences (labeled by Framework I). The other one is to find representative feature correspondences from 2D images and given a prior shape model then reconstructing the 3D surface by interpolation (labeled by Framework II). The first framework of reconstruction technique is similar to the correlation-based one due to the establishment of pixel-to-pixel correspondence which has drawbacks of low accuracy and high time complexity. This paper thus studied reconstruction technique by following Framework II. Based on Framework II, this paper focused on investigating the influence of feature correspondences establishment to 3D reconstruction accuracy for close-range objects. The model of the proposed 3D reconstruction model is shown in Fig. 4.

3 Criteria for Close-Image Objects Reconstruction

Fig. 5 shows an example of the reconstruction result based on the model given in Fig. 4. It can be seen that the correspondences established on the objects are almost contour or corner points labeled manually. It is invalid for close-range objects without contour or corner points on them, which raises problems of the selection of representative features for correspondence establishment. Meanwhile, the number and distribution of feature correspondences also plays an important role in the 3D

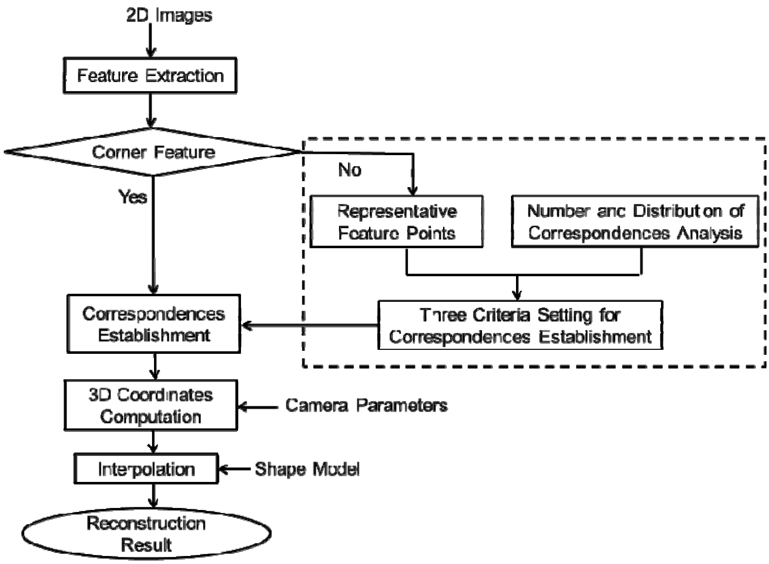

Fig. 4. The proposed 3D reconstruction model in this paper.

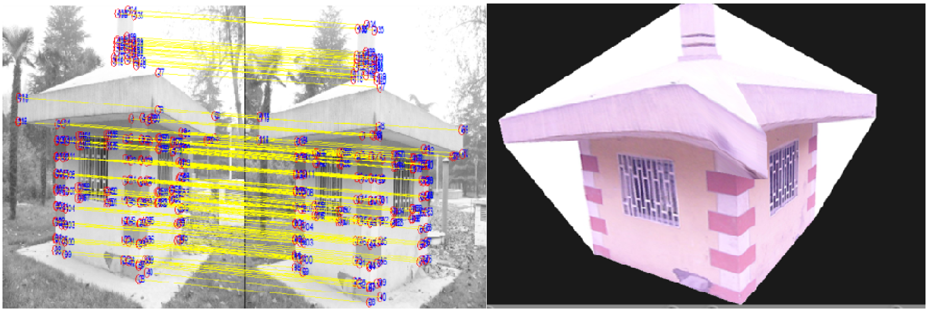

(a) (b)

Fig. 5. Building reconstruction results by following the model shown in Fig. 4. (a) contour or corner correspondences establishment result, (b) 3D reconstruction result wrapped with texture image.

reconstruction accuracy. These two problems are studied in-depth in the following subsections. Finally, three criteria are set based on the previous analysis so as to guide feature correspondences establishment for 3D modeling of close-range objects.

3.1 Selection of Representative Features for Correspondence Establishment

Generally speaking, it is intuitive that corner points which refers to the intersection of two lines or point which located in two adjacent objects with different principle lines will be selected as representative features for correspondence establishment, as the points manually labeled in Fig. 5. However, there are no corner points in some objects, as the example images shown in Fig. 2. It is necessary to find representative feature points or corner-like points to instead corner points for correspondence establishment. By observing the images of objects in Fig. 2, we can see that lines or regions of variation are widespread in them. In this paper, we assume the points located in the position with changes as representative feature points. There are three typical situations (e.g. on line, between lines, between regions) we summarized as follows.

The first two situations are relative to lines, which are for a single line and between lines. These two situations are analyzed based on fingerprint images since they consist of lines. As the solid line labeled in the example fingerprint image shown in Fig. 6, for a single line, it can be seen that changes occur in the end of the line or the point where its direction changes largely. Generally, the end of a line is defined as termination point (triangle labeled in Fig. 6) and the point where lines' direction largely changed refers to local extreme point (circle labeled in Fig. 6). Thus, such two kinds of points are selected as representative feature points for a single line in this paper. In the situation of between lines (see dashed lines labeled in Fig. 6), change just exist in the intersection point of lines, the representative feature point is then defined as the intersection point between lines (rectangle labeled in Fig. 6).

The third situation is between regions. Besides lines, some objects consist of different regions, as the iris image shown in Fig. 7. It can be seen that it contains regions with different textures and colors. Similar to the situation between lines, changes occurs in the boundary between adjacent regions, as circles labeled in Fig. 7. Thus, in the third case, representative feature points are defined as the points in the boundary between adjacent regions.

Finally, we summarize the first criterion for feature correspondences establishment to the 3D reconstruction of close-range objects as: *Criterion 1: selecting representative feature points or corner-like points for correspondence establishment.*

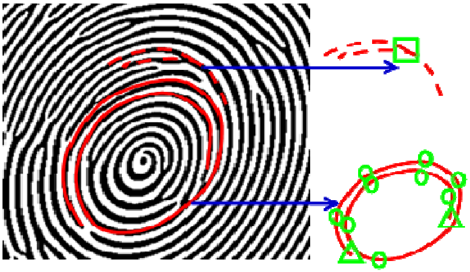

Fig. 6. Illustration of representative feature points of lines in a fingerprint image.

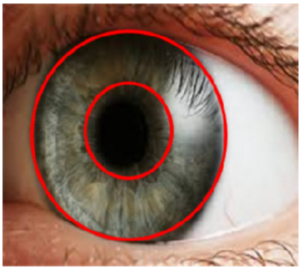

Fig. 7. Illustration of representative feature points between regions in an example iris image.

3.2 Influence Analysis of Correspondences to Reconstruction Accuracy

As known to everyone, it is extremely difficult to establish pixel-to-pixel feature correspondences manually or automatically, especially for close-range objects due to their small size and the unknown number and irregular distribution of feature points on them. To the best of our knowledge, there are no literatures available about the influence analysis of number and distribution of feature correspondences to 3D reconstruction accuracy. This subsection thus studied this problem by reconstructing a small object with standard cylinder shape and of radius 10mm. To facilitate the labeling of feature correspondences, we wrapped the cylinder with a grid paper, as shown in Fig. 8(a). As the representative feature points defined in the previous subsection, those feature points which are located in the boundary between adjacent regions are manually labeled for correspondence establishment. By following the method introduced in Section 2, the shape of the cylinder can be reconstructed. Here, a 3D software was used for the display and analysis of reconstruction results. This software is popularly used for 3D point cloud data display and analysis.

First, experiments were organized to analyze the effect of the number of correspondences on 3D reconstruction accuracy. Thus, the distributions of selected feature correspondences were all even. The largest number of correspondences between two 2D images shown in Fig. 8(b) is set to 40 for the reason that this is the largest area those points covered in the experiments. The number of feature correspondences both along horizontal axis and vertical axis was gradually reduced to get different reconstruction results. Table 1 lists the setting of parameters in the experiments, such as the number of feature correspondences, the distribution of correspondences, and the sampling interval and direction along decreasing number. The reconstruction results were also summarized in Table 1. Details of the corresponding feature correspondences establishment and reconstruction results were given in Fig. 9. From the results, we can see that the reconstruction accuracy dropped with the decreasing of correspondence number. From Tabel 1, we can see that there is a little influence of number decreasing on reconstruction accuracy for a line shape (vertical axis). For a curved shape (horizontal axis), the accuracy decreased when correspondence number decreasing and sampling interval increasing. For the same number of feature correspondences, the closer between correspondences, the larger the error may be due to the effect of errors resulted in 3D coordinate calculation for each correspondence.

Therefore, we set the second criterion for feature correspondences establishment to the 3D reconstruction of close-range objects as: *Criterion 2: Densely sampling of feature correspondences along the direction where depth changed quickly and sparsely sampling of feature correspondences along the direction where depth smoothly changed.*

We also conducted an experiment of 3D reconstruction by randomly selecting feature correspondences with irregular distributions. The selected feature correspondences and its reconstruction result are shown in Fig. 10, where the number of correspondences is around 20. By comparing the result with Enum-2, Enum-3 and Enum-4 shown in Fig. 8 (they have similar number of correspondences), we can see that better results were achieved with large sampling interval no matter the distribution of feature correspondences is even or not. Thus, the third criterion for feature correspondences establishment to the 3D reconstruction of close-range objects in this paper is: *Criterion 3: Establishing feature correspondences to cover the surface of object as large as possible.*

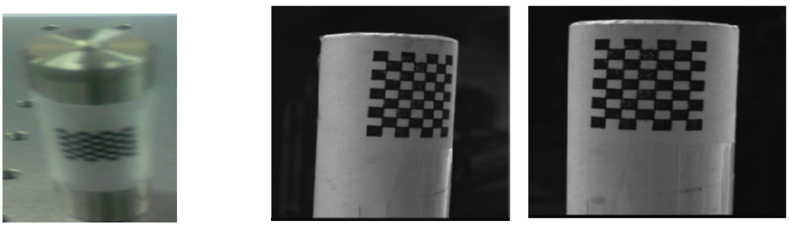

(a) (b)

Fig. 8. (a) Original cylinder shape object wrapped with grid paper, (b) 2D images of (a) captured by the left and right cameras in the experiments.

Table 1. Setting of experimental parameters and the corresponding reconstruction results.

Title of experiments	Enum-1	Enum-2	Enum-3	Enum-4	Enum-5	Enum-6	Enum-7	Enum-8	Enum-9
Number of feature correspondences	40	24	24	20	15	12	12	12	10
Distribution of correspondences	Even	Even	Even	Even	Even	Even	Even	Even	Even
(Sampling interval, Direction along decreasing number)	(2mm, -)	(4mm, horizontal)	(2mm, horizontal)	(4mm, vertical)	(6mm, vertical)	(6mm, horizontal)	(8mm, vertical)	(8mm, horizontal)	(10mm, vertical)
Reconstruction Radius (standard 10*mm*)	9.91	9.85	9.08	9.78	9.80	2.77	9.68	3.69	9.71

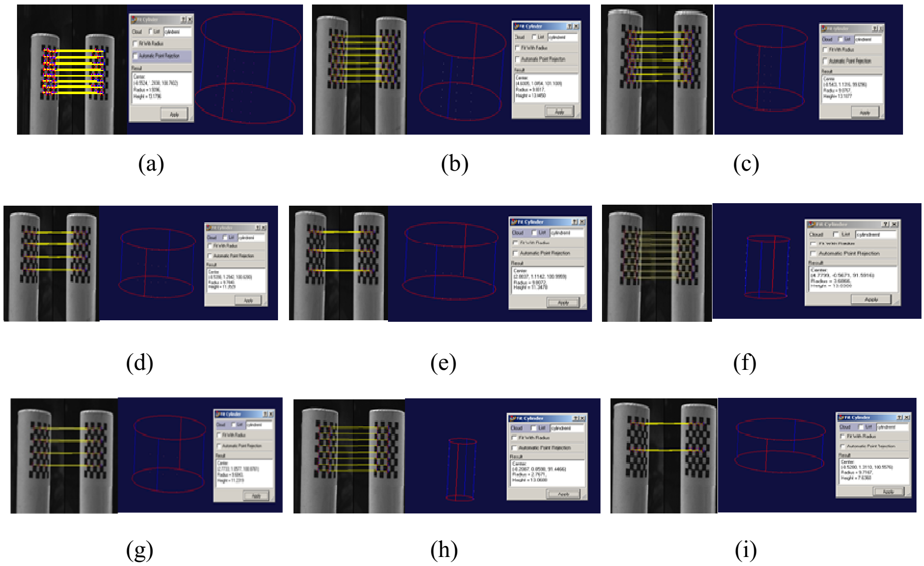

Fig. 9. Established feature correspondences and the reconstruction result for (a) Enum-1, (b) Enum-2, (c) Enum-3, (d) Enum-4, (e) Enum-5, (f) Enum-6, (g) Enum-7, (h) Enum-8, (i) Enum-9, listed in Table 1.

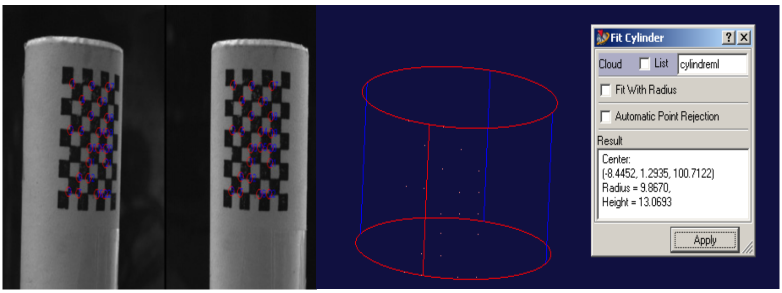

Fig. 10. Established feature correspondences with irregular distribution and the reconstruction result.

4 Case Study: Application to Human Finger

As we can see that human fingers are typical close-range objects. To verify the effectiveness of the proposed reconstruction model and the criteria to the reconstruction accuracy for close-range objects, this paper took the reconstruction of finger shape as a case study. The device used to capture 2D fingerprint images was the same as the one introduced in Ref. [35].

4.1 Effectiveness Validation of the Proposed Reconstruction Model

As mentioned in Section 2, there are two frameworks to realize 3D results by using feature-based reconstruction technique. The paper selected Framework II in the proposed reconstruction model. This subsection tries to demonstrate the effectiveness of the proposed model by reconstructing a human finger with two frameworks mentioned in Section 2. First, we manually labeled 50 representative feature correspondences on example fingerprint images by following the criteria set in Section 3, as shown in Fig. 11(a). Then, pixel-to-pixel correspondences were established by estimating the transformation model between images based on previously labeled feature correspondences. The result is shown in Fig. 11(b). Here, the rigid transform was selected as the model between images. After that, 3D reconstruction results can be achieved by following the procedures given in Section 2, as shown in Fig. 12. For better comparison, the depth of the reconstruction result is normalized to [0, 1] by MIN-MAX rule. From Fig. 12, we can see that the result obtained by the proposed model is closer to the appearance of human finger than the one generated by following the procedure of framework I.

Furthermore, we compared the reconstruction results with the 3D point cloud data of the same finger to verify the effectiveness of the model. The 3D point cloud data are defined as the depth information of each point on the finger. They are collected by a camera together with a projector using the Structured Light Illumination (SLI) method [36, 37]. Since this technique is well studied and proved to acquire 3D depth information of each point on the finger with high accuracy [36, 37], 3D point cloud data obtained using this technique are taken as the ground truth of the human finger in this paper. Compared our results in Fig. 12 with the ground truth shown in Fig. 13, it can be seen that the profile of the human finger shape reconstructed based on the proposed model is similar to the 3D point cloud data even though it is not that accurate. Meanwhile, the reconstruction result based on framework I shown in Fig. 12(a) is quite different from the 3D point cloud data. The real distances between the upper left core point and the lower left delta point of the reconstruction results in Fig. 12(a) and Fig 12(b), as well as of the ground truth in Fig. 13(a) were also calculated. The corresponding values are 0.431, 0.353 and 0.386, respectively. As a result, it is concluded that the proposed model is effective even though there is an error between the reconstruction result and the 3D point cloud data.

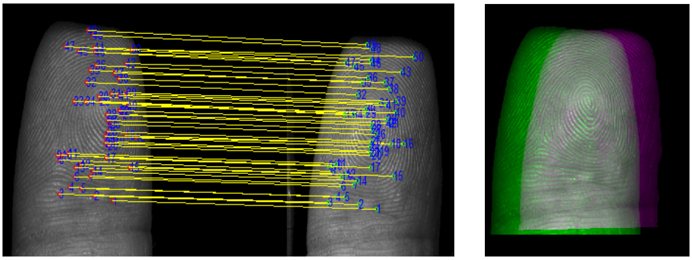

(a) (b)

Fig. 11. Correspondences establishment results. (a) manually labeled 50 presentative feature correspondences, (b) pixel-to-pixel correspondences (gray part in the center) after rigid transformation between fingerprint images.

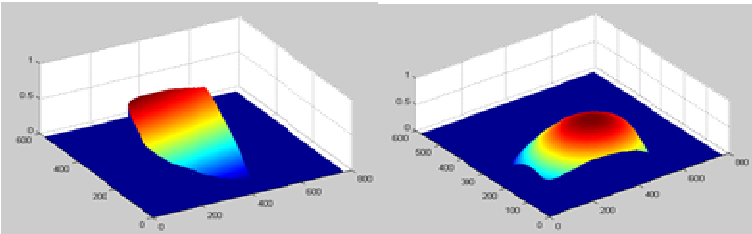

(a) (b)

Fig. 12. 3D reconstruction results. (a) reconstruction result based on the model of Framework I, (b) reconstruction result based on our proposed reconstruction model.

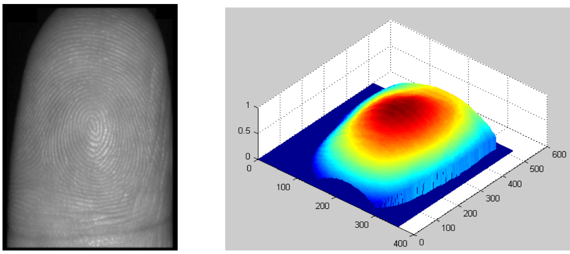

(a) (b)

Fig. 13. Ground truth of the same finger of Fig. 11 captured by structured light illumination (SLI) technique. Comparison of 3D fingerprint images from the same finger but different acquisition technique: (a). original fingerprint image captured by the camera when collecting 3D point cloud, (b). 3D point cloud collected by one camera and a projector using the SLI method.

Table 2. Reconstruction results from different fingerprint feature correspondences of Fig. 11.

Results / Used feature	Established correspondences	Reconstructed 3D fingerprint image
Minutiae	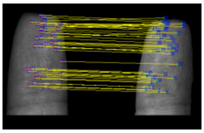	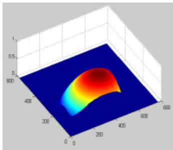
Ridge feature	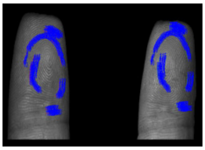	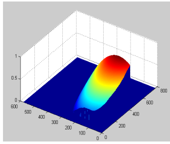

4.2 Criteria Verification

This paper proposed three criteria to guide feature correspondences establishment for the 3D reconstruction of close-range objects. The effectiveness of such criteria was verified by analyzing the reconstruction accuracy based on different fingerprint feature correspondences. As studies in [38], there are two classical fingerprint features for low resolution fingerprint images, namely ridge feature and minutiae. Feature correspondences were first established automatically from the images shown in Fig. 11 by using the algorithms introduced in [35, 38, 39], and then the reconstruction results were generated based on those three different fingerprint feature correspondences, as illustrated in Table 2. It can be seen that the results are different corresponding to different feature matched pairs due to different numbers and distribution of established fingerprint feature correspondences and also the existence of false correspondences.

From the results shown in Table 2, it can be seen that the reconstruction result based on minutiae correspondences is better than the one based on ridge feature. The histograms of error maps between the results in Table 2 and the ground truth in Fig. 13(b) are shown in Fig. 14. Smaller errors were achieved between the minutiae-based reconstruction result and the ground truth. These results fully demonstrated the proposed criteria in this paper that: (1) minutiae, which refer to the ends or bifurcations of ridges, are satisfied the definition of representative feature points or corner-like points in the paper. However, ridge feature, which is the sampling of lines, provides too much insignificant information. Thus, it is better to select representative feature points or corner-like points for correspondence establishment; (2) poor result will be achieved if densely establishing correspondences along the direction with smoothly changed depth, like ridge feature correspondences. Therefore, we recommended to sparsely sampling of feature correspondences along the direction where depth smoothly changed; (3) the region covered by minutiae correspondences is larger than the one covered by ridge correspondences, better reconstruction result is achieved correspondingly. Hence, this paper set the third criterion for feature correspondences establishment to cover the surface of object as large as possible.

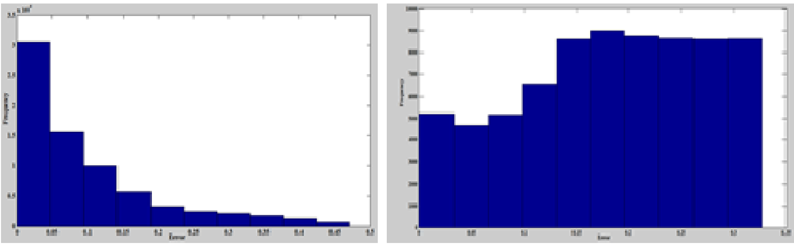

(a) (b)

Fig. 14. Histogram of error maps between reconstructed results in Table 2 and Fig. 13(b). (a) histogram of err map between Fig. 13(b) and reconstruction result by using minutiae, (c) histogram of err map between Fig. 13(b) and reconstruction result by using ridge feature.

5 Conclusion

The issue of feature-based 3D reconstruction method for close-range objects was investigated in this paper. For close-range objects, it is very hard to found pixel-to-pixel correspondence from their 2D images. Thus, our study mainly focused on 3D modeling with limited feature correspondences. In this situation, the selection of representative feature correspondences, the number and distribution of the feature correspondences play an important role in the 3D reconstruction accuracy. Then, features on representative close-range objects were analyzed and the suitable features for correspondence establishment were indicated. Subsequently, the impact of the number and distribution of feature correspondences was analyzed by reconstructing an object with standard cylinder shape and of radius 10mm. Three criteria were set to guide the selection of features on close-range objects for more accurate 3D reconstruction. We finally took the reconstruction of human finger as a case study by applying our setting criteria. The effectiveness of the setting criteria was demonstrated by comparing the accuracy of reconstructed finger shape based on different fingerprint feature correspondences with the corresponding 3D point cloud data obtained by structured light illumination (SLI) technique which was taken as a ground truth in the paper.

Acknowledgement. The authors would like to thank the editor and the anonymous reviewers for their help in improving the paper. The work is supported by the NSFC fund 61403257 and Natural Science Foundation of SZU 201532.

References

1. Rusinkiewicz, S., Holt, O., Levoy, M.: Real-time 3D model acquisition. In: The Proceedings of the 29th Annual Conference on Computer Graphics and Interactive Techniques, no. 3, vol. 21, pp. 438–446, July 2002
2. Bradley, B., Chan, A. , Hayes, M.: A simple, low cost, 3D scanning system using the laser light-sectioning method. In: IEEE International Instrumentation and Measurement Technology Conference Victoria, Vancouver Island, Canada, pp. 299–304, May 2002

3. Wu, Q., et al.: A 3D modeling approach to complex faults with multi-source data. Computers & Geosciences **77**, 126–137 (2015)
4. Wang, Y., Hassebrook, L., Lau, D.: Data acquisition and processing of 3-D Fingerprints. IEEE Transactions on Information Forensics and Security **5**(4), 750–760 (2010)
5. Stockman, G., Chen, S., Hu, G., Shrikhande, N.: Sensing and recognition of rigid objects using structured light. IEEE Control Syst. Mag. **8**(3), 14–22 (1988)
6. Hu, G., Stockman, G.: 3-D surface solution using structured light and constraint propagation. IEEE Trans. Pattern Anal. Mach. Intell. **11**(4), 390–402 (1989)
7. Horn, B.: Shape from shading: A method for obtaining the shape of a smooth opaque object from one view. Technical Report No. 232, AI Lab., MIT (1970)
8. Zhang, R., Tsai, P., Cryer, J., Shah, M.: Shape from shading: A survey. IEEE Transactions on Pattern Analysis and Machine Intelligence **21**(8), 690–706 (1999)
9. Worthington, P.: Reillumination driven shape from shading. Computer Vision and Image Understanding **98**(2), 326–344 (2005)
10. Akimoto, T., Suenaga, Y., Wallace, R.: Automatic creation of 3D facial models. IEEE Computer Graphics & Applications **13**(5), 16–22 (1993)
11. Lao, S., Sumi, Y., Kawade, M., Tomita, F.: Building 3D facial models and detecting face pose in 3D space. In: Proc. of Second Int. Conf. on 3D Digital Imaging and Modelling, pp. 398–404 (1999)
12. Brodski, T., Fermuller, C., Aloimonos, Y.: Shape from video. IEEE Computer Society Conference on Computer Vision and Pattern Recognition **2**, 1–151 (1999)
13. Strecha, C., Verbiest, F., Vergauwen, M., Van Gool, L.: Shape from video vs. still images. In: Proceedings Conference on Optical 3D Measurement Techniques, Zürich, Switzerland, vol. 2, pp. 168–175 (2003)
14. Woodham, R.: Photometric method for determining surface orientation from multiple images. Optical Engineering **19**(1), 139–144 (1980)
15. Rushmeier, H., Taubin, G., Gueziec, A.: Applying shape from lighting variation to bump map capture. In: Proc. of Eurographics Work. on Rendering, St. Etienne, France, pp. 35–44 (1997)
16. Malzbender, T., Wilburn, B., Gelb, D., Ambrisco, B.: Surface enhancement using real-time photometric stereo and reflectance transformation. In: Eurographics Workshop on Rendering, Switzerland, pp. 245–250 (2006)
17. Grün, A.: Semi-automated approaches to site recording and modeling. Int. Archives of Photogrammetry and Remote Sensing **33**(B5), 309–318 (2000)
18. Bradley, B., Chan, A., Hayes, M.: A simple, low cost, 3D scanning system using the laser light-sectioning method. In: Proceedings of the IEEE International Instrumentation and Measurement Technology Conference Victoria, Vancouver Island, Canada, pp. 299–304, May 2002
19. Paris, S.: Methods for 3D reconstruction from multiple images
20. Said, A., Halabi, H., Baharum, B.: Image-based modeling: a review. Journal of Theoretical and Applied Information Technology, 188–196 (2005)
21. Remondino, F., El-Hakim, S.: Image-based 3D modeling: A review. The Photogrammetric Record **21**(115), 269–291 (2006)
22. Divya, U.J., Kim, H.S., Kim, J.I.: An image-based approach to the reconstruction of ancient architectures by extracting and arranging 3D spatial components **16(**1), 12–27 (2015)
23. Grün, A., Remondino, F., Zhang, L.: Photogrammetric reconstruction of the Great Buddha of Bamiyan, Afghanistan. The Photogrammetric Record **19**(107), 177–199 (2004)

24. Xia, S., Zhu, Y.: 3D simulation and reconstruction of large-scale ancient architecture with techniques of photogrammetry and computer science. In: CIPA 2005 XX International Symposium, Torino, Italy (2005)
25. Zhang, R., Tsai, P., Cryer, J., Shah, M.: Shape-from-shading: a survey. IEEE Transactions on Pattern Analysis and Machine Intelligence **21**(8), 690–706 (1999)
26. Poggio, G., Poggio, T.: The analysis of stereopsis. Annual Review of Neuroscience **7**(1), 379–412 (1984)
27. Hartley, R., Mundy, J.: The relationship between photogrammetry and computer vision. In: Barrett, E.B., McKeown, D.M. (eds.) SPIE Proceedings. Integrating Photogrammetric Techniques with Scene Analysis and Machine Vision, vol. 1944, pp. 92–105. SPIE Press (1993)
28. Henrichsen, A.: 3D reconstruction and camera calibration from 2D Images. University of Cape Town (2000)
29. Hartley, R.: Multiple view geometry in computer vision. Cambridge Univ. Press, Cambridge (2000)
30. Zhang, Z.: A flexible new technique for camera calibration. IEEE Trans. on Pattern Anal. Mach. Intell. **24**(11), 1330–1334 (2000)
31. Bouguet, J.: Camera Calibration Toolbox for Matlab
32. http://en.wikipedia.org/wiki/Correspondence_problem#Basic_Methods
33. Ogale, A., Aloimonos, Y.: Shape and the stereo correspondence problem. International Journal of Computer Vision **65**(3), 147–162 (2005)
34. Belhumeur, P., Mumford, D.: A bayesian treatment of the stereo correspondence problem using half-occluded regions. In: IEEE Computer Society Conference on Computer Vision and Pattern Recognition, pp. 506–512 (1992)
35. Liu, F., Zhang, D., Song, C., Lu, G.: Touchless Multi-view Fingerprint Acquisition and Mosaicking. IEEE T. Instrumentation and Measurement **62**(9), 2492–2502 (2013)
36. Wang, Y., Hassebrook, L., Lau, D., Data acquisition and processing of 3-D Fingerprints, IEEE Transactions on Information Forensics and Security, **5**(4), 750–760 (2010)
37. Zhang, D., Kanhangad, V., Luo, N., Kumar, A.: Robust palmprint verification using 2D and 3D features. Pattern Recognition **43**(1), 358–368 (2010)
38. Choi, H., Choi, K., Kim, J.: Mosaicing touchless and mirror-reflected fingerprint images. IEEE Trans. On Information Forensics and Security **5**(1), 52–61 (2010)
39. Jain, A., Hong, L., Bolle, R.: On-line fingerprint verification. IEEE Trans. on Pattern Anal. Mach. Intell. **19**(4), 302–314 (1997)